

# In-Situ Non-Destructive Evaluation of Ultrasonic Additive Manufactured Components

Venkata Karthik Nadimpalli<sup>1, (a)</sup>, Jeong K. Na<sup>2</sup>, Darren T. Bruner<sup>3</sup>, Brenna A. King<sup>3</sup>, Li Yang<sup>1</sup>,  
Brent E. Stucker<sup>4</sup>

<sup>1</sup> *Department of Industrial engineering, J.B Speed School of Engineering, University of Louisville,  
Louisville, Kentucky*

<sup>2</sup> *Advanced NDI, Aerospace Group, Wyle Laboratories Inc., 2700 Indian Ripple Road, Dayton, Ohio*

<sup>3</sup> *Department of Mechanical engineering, J.B Speed School of Engineering, University of Louisville,  
Louisville, Kentucky*

<sup>4</sup> *3D SIM LLC*

a) Corresponding Author: knadimpalli18@gmail.com

**Abstract.** In-situ monitoring of Ultrasonic Additive Manufacturing (UAM) process is crucial for producing parts suitable for load-bearing structural applications. Due to the nature of UAM process, it is necessary to monitor the entire build as opposed to only the just bonded layer. For this purpose, an ultrasonic transducer is used in this study to perform in-situ nondestructive evaluation (NDE) of the entire build after the addition of each new layer. This has been successfully implemented first on a manually operated research UAM machine and then applied on a fully automated commercial grade UAM machine. The practical applications of such in-situ measurements for ensuring defect-free part fabrication through closed-loop control of the UAM process control is shown to be possible from the results of this work.

## INTRODUCTION

UAM is a layer by layer metal based solid state bonding process [1] which is commonly used in conjunction with a CNC mill and offers advantages in material properties as compared to traditional metal joining and forming technologies [2]. In this process, a high level of ultrasonic energy is utilized to create solid state metallurgical bonding between a thin foil and an existing base. Given the right process parameters, 100% linear weld density can be achieved. CNC machining after depositing each layer is done to achieve required shapes and dimensions, enabling a freeform fabrication. The additive-subtractive nature and the low-heat solid state processing give the UAM process certain unique capabilities such as completely enclosed internal cooling channels, smart parts with embedded sensors and metal-matrix composites that cannot be produced otherwise [3-5]. Even dissimilar metals that are not metallurgically compatible can be combined to produce multi-material parts without any embrittlement or cracking problems. For several years, the material systems that could easily be bonded using the UAM process were limited to aluminum alloys due to very high ultrasonic power requirement for other engineering alloy materials. Newer, commercial grade UAM systems overcome this hurdle by using a high power transducer and load

cell, which makes it possible to build components from titanium, nickel and iron based alloy systems [6]. Figure 1(a) shows a schematic of the UAM process and Figure 1(b) shows the manual research machine used in the current study. The load cell shown in Figure 1(b) applies a constant force while the ultrasonic horn laterally vibrates as it moves forward causing intense plastic deformation at the foil/substrate interface forcing the foil to bond to the substrate. The process of ultrasonic bonding involves breaking up of oxide layers on the surface of the sheet metal, followed by nascent metal contact due to intense plastic deformation. Normally, UAM components are transversely anisotropic along the build direction by nature as they are layered composite structures. The quality of bonding at each interface determines the overall component strength. Since UAM was developed for producing end-use functional parts, it is beneficial to monitor the process online to enable closed loop control of the process.

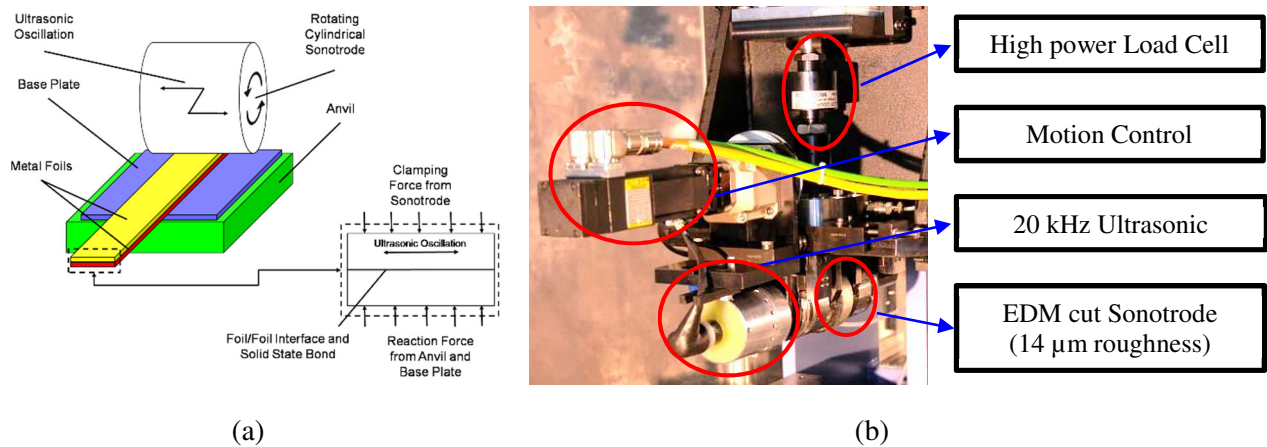


**FIGURE 1.** (a) Schematic of the Ultrasonic Additive Manufacturing consolidation process and (b) SonicLayer R200 manually operated research machine.

## MOTIVATION

UAM parts may contain several defects such as partial and kissing bonds (even complete delamination) unless the process parameters are continually changed with increasing build height. This is because layer bonding is a vibration dependent phenomenon. During each welding cycle, the entire part vibrates under a compressive load. This can lead to opening of any kissing bonds or partial bonds into delamination. Thus, it is imperative to ensure that not only the current layer is fully consolidated, but also all the previously bonded layers are intact. This is not as critical with other additive processes such as selective laser melting where it is enough to monitor the top surface of the build using optical techniques such as infrared imaging. But in the case of UAM, a layer may be fully bonded initially, but can develop into a delamination due to repeated cyclic loading several layers after it has been bonded. It is thus crucial to have a monitoring mechanism that can see through the entire component. Sometimes, IR cameras are used to monitor the top surface of the UAM build [7] or embedded thermocouples are used to measure the temperature within the part [8]. Both these approaches, while having their merits, are not intended nor are thought to be suitable for online monitoring. In this study, conventional longitudinal mode broadband ultrasonic contact transducers are utilized to take a single point scan after each layer is deposited.

## METHOD

### *In-Situ Ultrasonic Non-Destructive Evaluation Setup*

The sonotrode employed in the current study has a surface roughness of  $14\ \mu\text{m}$  and it gives an average surface roughness of around  $10\ \mu\text{m}$  on the top of each deposited layer. The first in-situ monitoring system design involved a setup that can scan the part from the top as shown in Figure 2 (a). It was soon realized that performing an ultrasonic scan over the part after each layer was not practical due to unintended interruption to the manufacturing process itself. Thus, a new system was designed to provide access from below the base plate as shown in Figure 2 (b). This setup allows for the user to have a capability of continuous monitoring for the NDE signals without any interruption during part fabrication. The preliminary setup was designed to be a single point normal incident contact measurement aimed at the middle of the build area. [9] has used a similar setup with access from below to measure laser melted AM components using ultrasonic sensors

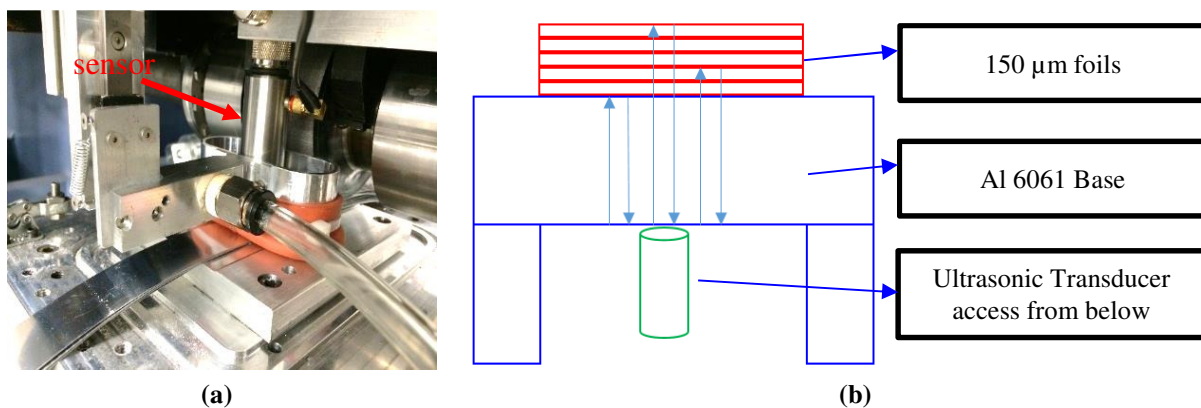


**FIGURE 2.** (a) C-Scan immersion acoustic microscopy approach with access from the top and (b) schematic of in- situ setup with access from below the base plate.

### *Factorial Design of Experiments*

For the current online monitoring study,  $150\ \mu\text{m}$  Al 6061 H18 foil was chosen. While the processing parameters for Al 6061 have been well established using the Solidica Ultrasonic Consolidation system [10-11], the higher power UAM system provides a wider range of possible process parameters. Two sets of experiments were performed with similar bonding parameters, one on a manually operated research machine and another on a fully automated commercial grade machine. To study the feasibility of in-situ measurements, an ultrasonic NDE setup was first designed and installed on the research machine. The controllable parameters in UAM are applied force (F), velocity of bonding (V) and amplitude of vibration (A). Of these three parameters, the effect of amplitude is most significant. Varying all three parameters together requires a large number of samples to statistically separate the coupled effects of the build parameters. Hence, in this study, force and velocity were kept constant and only amplitude was changed. A three replicate amplitude factorial was carried out on the SonicLayer R200 machine at a constant force of 5000 N (1120 pounds) and a constant velocity of 85 mm/s (200 inch per minute). Rectangular specimens with flat top surface measuring 1" x 3" with a built height of 45 layers were manufactured. In each replicate the amplitudes had 6 values ranging from 27 - 47  $\mu\text{m}$ . Based on the data gathered from the research machine, the range of amplitudes was readjusted to be 25 - 35  $\mu\text{m}$  for the subsequent measurements on a commercial grade Fabrisonics SonicLayer 7200 UAM machine.

### In-Situ Data Acquisition

A 5 MHz longitudinal mode broadband contact transducer was driven using a JSR Ultrasonics, DPR 500 remote pulser/receiver module. Ultrasonic data was processed by using a 1.5 GHz 14-bit Acquisition Logic PCI digitizer A 500 V negative pulse was used to drive the transducer with a damping of  $50 \Omega$  at a pulse repetition rate of 200 Hz. The processed raw ultrasonic data was exported and analyzed in MATLAB. Figure 3 shows A-Scan signals collected on the base (before depositing any layers), after 5 layers, and after 10 layers of UAM builds. It can be observed that the signal starts shifting to the right as the build height increases. It is also clear that the reflections from the interface are significantly small. In this study, measurements were only taken after building each layer. It should be noted that each interface goes through several cycles of load as more layers are built. Of all the interfaces in the build, the very first interface formed between the base and the UAM build is of primary importance. Delamination of the first interface during manufacturing may ruin the part. Due to the nature of the loading condition in the UAM system, the base/build interface tends to be the weakest link as it experiences the maximum shear loads on account of being farthest from the Sonotrode head. Often times the base is used as a part of the final part or component. In such cases, it becomes critical to have a sound base/build interface.

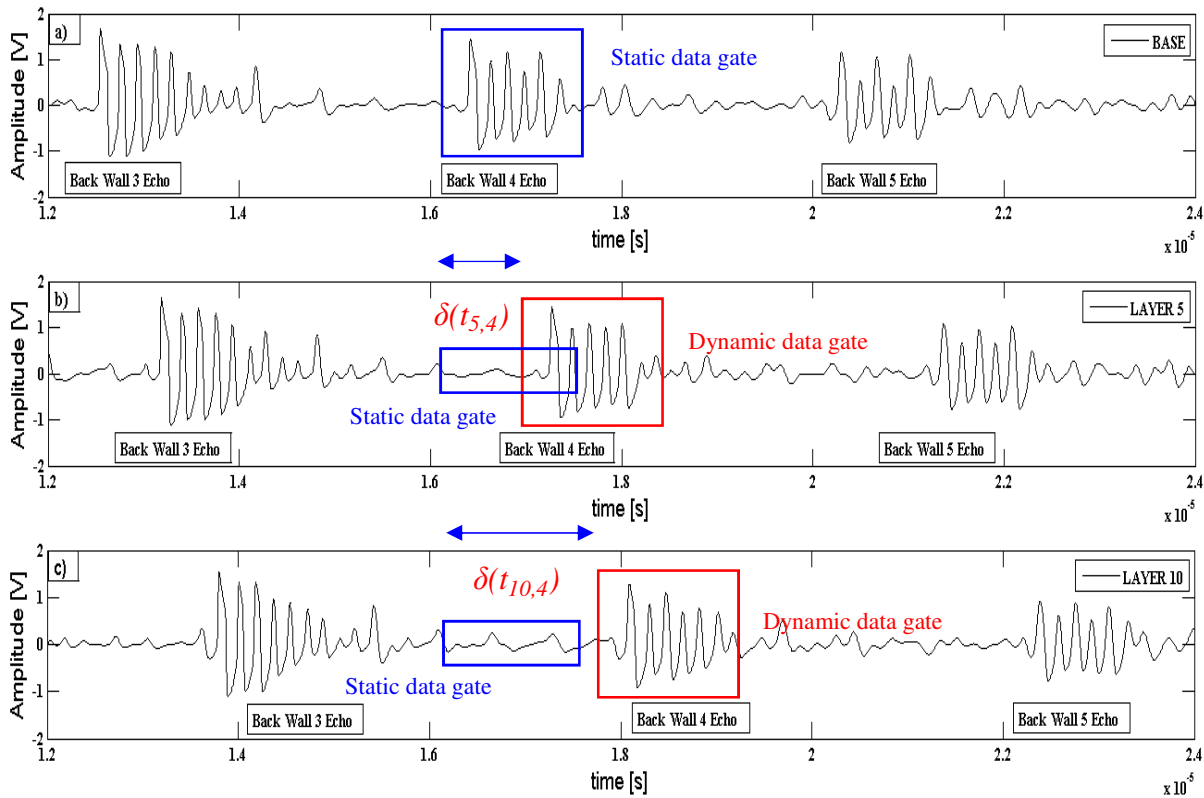
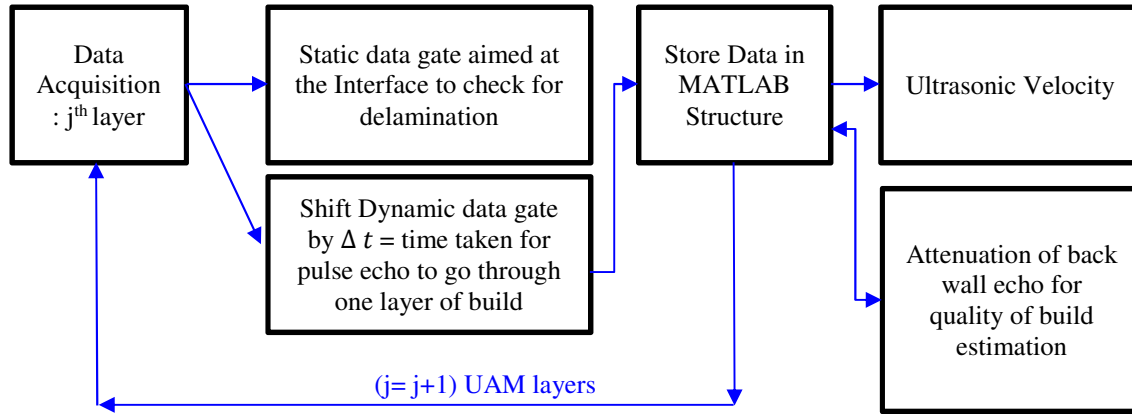


FIGURE 3. Shift in the time of flight of back wall echoes as new layers are added.

### Data Analysis

A total of 18 test specimens, 45 layers in each, were built. During manufacturing, ultrasonic data was collected one per layer. Analysis of all this data was carried out by importing each of these waveforms into MATLAB.



**FIGURE 4.** Logic used for data acquisition and analysis.

The two crucial data sets in the A-Scan signals are the interface reflection (the initial position of the peak on the base) and the current top surface echo (i.e., base plus build). To be able to analyze data in the far field, the back wall 3 and 4 echoes from the top of the build were investigated. As a new layer is added, two data gates of information are stored in a MATLAB structure, the first one being the region around where the interface peak is expected (depending on base plate thickness), and the second one being the shift in the data gate of a specific echo so as to capture the essential echo waveform. This shift is different for back wall 3 and back wall 4 due to different travel times. This moving data gate always captures the back wall echoes (i.e. the reflection from the top of the specimen) and the static data gate captures any reflections from the interface as shown in Figure 3. Storing all the echo waveform data in a MATLAB structure helps easily form correlations between different build parameters and between different layers of the same build.

### ***Ultrasonic Velocity and Attenuation***

Linear ultrasonic parameters that can be readily calculated from a time domain signal are ultrasonic velocity and attenuation. Accurate calculation of ultrasonic velocity requires knowledge of the thickness of the component that is being measured. The correlation between ultrasonic velocity and mechanical properties is well known. The extent of consolidation of a foil depends on the input parameters used. Due to the large amount of plastic deformation and loads applied, the foil thickness reduces after bonding. The average thickness value of each layer is dependent on the process parameters used. In the current study, the thickness of the builds consisting of 45 layers was measured to obtain the average layer thickness for each of the parameter sets.

To find the time delay due to the addition of a new layer of UAM build, two approaches can be followed. The first one involves choosing two/three consecutive back wall echoes of a single waveform and finding the group delay between them. The second approach involves choosing a back wall echo in the far field and following the time shift in that back wall echo due to the addition of a new layer. The advantage of the second method is that all measurements are performed relative to the base material which is acting like a buffer rod. Such a buffer zone is helpful to measure the change due to a small thickness addition as shown by Papadakis [12]. This also eliminates the effect of coupling and the phase shift associated with it. Thus, the second approach has been chosen

as a suitable analysis method for the current study. Ultrasonic group velocity was calculated according to equations 1 and 2, and ultrasonic attenuation according to equation 3.

$$T_{j,N} = t_{max} \left[ \text{abs} \left( \text{Hilbert} \left( \text{Wave}_{j,N} \right) \right) \right] - t_{max} \left[ \text{abs} \left( \text{Hilbert} \left( \text{Wave}_{base,N} \right) \right) \right] + \delta(t_{j,N}) \quad (1)$$

$$V_{group,j,N} = \frac{2Njd_{param}}{T_{j,N}} \quad \delta(t_{j,N}) = \frac{2Njd_{param}}{C} \quad (2)$$

$$L_{j,N} = 20 \log \left( \frac{\text{Amp}(\text{FFT}_{j,N}(f_{trans}))}{\text{Amp}(\text{FFT}_{base,N}(f_{trans}))} \right) \quad (3)$$

$\text{Wave}_{j,N}$  is the data gate that captures the  $N^{\text{th}}$  back wall echo after  $j$  layers of UAM build and  $\delta(t_{j,N})$  is the time delay between the first static data gate and the  $j^{\text{th}}$  dynamic data gate as shown in Figure 3. The value of  $\delta(t_{j,N})$  is calculated from the known average layer thickness for a given parameter set  $d_{param}$ , the back wall echo number  $N$ , layer number  $j$ , and the velocity  $C$  for Al6061.  $t_{max}[\text{Wave}]$  represents the time at which the maximum of the rectified envelope signal occurs, which is used to calculate the group delay  $T_{j,N}$ .  $V_{group,j,N}$  is the group velocity through  $j$  layers of UAM build.  $L_{j,N}$  is the relative attenuation in dB due to the addition of new UAM layers.  $\text{Amp}(\text{FFT}_{j,N}(f_{trans}))$  represents the magnitude of the FFT of the  $\text{Wave}_{j,N}$  signal calculated at  $f_{trans}$  which is the center frequency of the transducer. The attenuation loss is calculated as a relative amplitude change of the center frequency component of the  $N^{\text{th}}$  back wall echo signal after  $j$  layers of build.

## RESULTS

### ***Delamination Detection and Parameter Estimation for the Research UAM Machine***

Three replicates of a large parameter set were built in the research machine to determine under what conditions the base/build interface starts separating. At a constant force of 5000 N (1120 Pounds) and a constant build velocity of 85 mm/s (200 Inch per minute), the amplitude of UAM builds was varied from 27 - 47  $\mu\text{m}$  on the research machine. Figure 5 shows how the static and dynamic data gates work to detect delamination for a typical case of 45  $\mu\text{m}$  vibration amplitude.

Until 8 layers of UAM build (1.2 mm height), the signal from the very top of the part seems to be the strongest and it moves in accordance with the dynamic data gate. By layer 10, signals started showing up on the static data gate. By layer 14, there is a clear and complete delamination at the center of the base/build interface which is large enough to reflect the entire signal back. This is also clear from the dynamic data gate as there is no transmission through the UAM build. After 23 layers, the build showed the first signs of visual delamination from the base while indications from online monitoring started as early as layer 10. It is evident that ultrasonic signals can detect an indication of delamination for the base/build interface much earlier than the damage stage at which delamination can be visually detected. This capability was used to search across a range of parameter sets to identify the amplitudes when the base/build interface bond breaks down hence limiting the ability of the in-situ ultrasonic monitoring system.

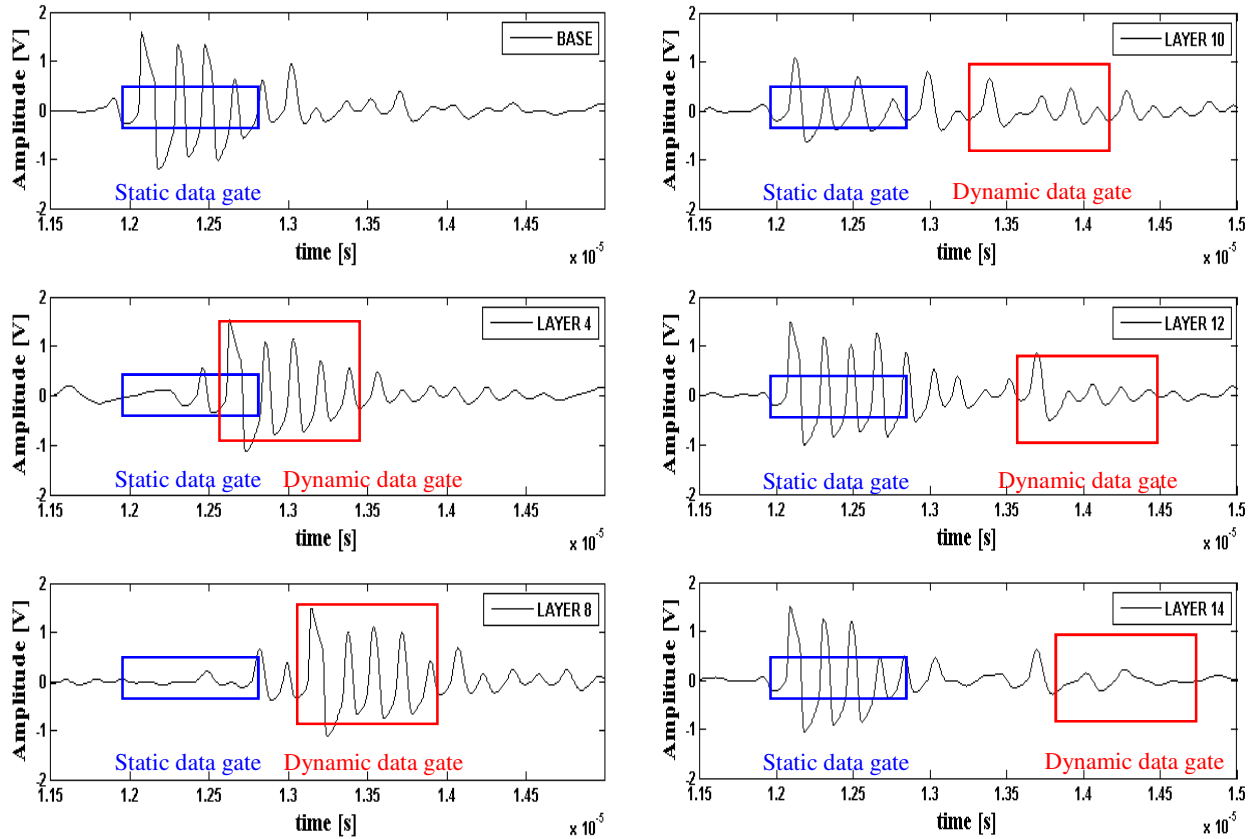


**FIGURE 5.** Delamination detection in a build with 45  $\mu\text{m}$  vibration amplitude. By using the static data gate coupled with the dynamic data gate, indications of delamination can be detected.

Table 1 shows the results across three replicates of the six factor amplitude factorial (27 - 45  $\mu\text{m}$ ) carried out on the research machine. It is observed that the components started delaminating at the base when increasing the amplitude above 35  $\mu\text{m}$ . In many cases, the delamination becomes visually observable several layers after it has been detected by ultrasound. When two out of three replicates delaminate from the base, such parameter sets are considered unsuitable. At a very high amplitude such as 47  $\mu\text{m}$ , the foils start sticking to the sonotrode, marking the upper limit of the amplitude. It is clear that amplitudes above 35  $\mu\text{m}$  are too harsh on the base/build interface for in-situ monitoring. Hence the parameters for building components on the commercial machine were chosen to be in the range of 25 to 35  $\mu\text{m}$  with increments of 2  $\mu\text{m}$ .

**TABLE 1.** Observations of base/build delamination during part fabrication on the research machine. The number in parentheses indicates after how many layers the delamination can be detected.

Amplitude	Replicate 1	Replicate 2	Replicate 3
27 $\mu\text{m}$	Good	Good	Good
31 $\mu\text{m}$	Good	Good	Good
35 $\mu\text{m}$	Good	Delamination (23)	Good
39 $\mu\text{m}$	Delamination (18)	Delamination (21)	Good
43 $\mu\text{m}$	Delamination (19)	Delamination (14)	Delamination (16)
47 $\mu\text{m}$	Delamination (7)	Delamination (10)	Delamination (12)



In the components built using the commercial machine, ultrasonic monitoring suggested delamination in two (33 and 35  $\mu\text{m}$  builds) out of eighteen parts although there were no visual indications. Unlike the manual research machine, with the automatic commercial machine, the trends in ultrasonic velocity and attenuation did not vary widely across the replicates for a given parameter set. Due to material sticking onto the surface of the UAM horn, uniform bond quality is often achieved after a thin layer of the material is formed on the horn which is called a patina. It is found that similar parameters can have different bond qualities if parts are manufactured using a fresh horn or a horn with a patina. After the formation of a good patina, in the third replicate of the factorial design, none of the components delaminated from the base and there were no outliers in the trends.

### ***Ultrasonic Group Velocity***

Ultrasonic group delay  $T_j$  as calculated by Equation 1 is always the cumulative effect of the  $j$  layers of UAM build on the delay of the ultrasonic signal. Hence, it gives the average group delay due to the current UAM build. The layer wise cumulative group delay is expected to increase linearly if one assumes that each layer has uniform bond quality. It has been observed that the group delay is largely dependent on the build parameters. The null hypothesis is to assume that the UAM builds are perfect and there is only a thickness change which causes the group delay. To test this hypothesis, the average thickness after bonding 45 layers has been measured with a vernier caliper. The average layer thickness was found to monotonically decrease from an average of 148  $\mu\text{m}$  for 25  $\mu\text{m}$  build amplitude to an average of 140  $\mu\text{m}$  for 35  $\mu\text{m}$  build amplitude. This is understandable as higher build amplitudes lead to more consolidation and plastic deformation, resulting in greater reduction in foil thickness. However, on the calculation of ultrasonic velocity from these thickness values, it was found that the null hypothesis is rejected and the change in group delay is due to imperfect interfaces within the components. Since accurate thickness values are not known for the first few layers, the group velocity calculations in Figure 6 are shown starting from layer 6 onwards. The group velocity values for amplitudes 25 and 27  $\mu\text{m}$  are calculated until the actual signal amplitude from the top of the UAM build drops to a value when it cannot be differentiated from reverberations within the part. This gives some spurious results which can be ignored. Also, once the component turns so bad that it highly attenuates the ultrasonic signal, it is no longer worth monitoring.

As can be seen in Figure 6, the group velocity clearly differentiates between various build amplitudes. It indicates that the 33 and 35  $\mu\text{m}$  builds are clearly the best. The 29 and 31  $\mu\text{m}$  builds are significantly better than the 25 and 27  $\mu\text{m}$  ones. Parts with 25 and 27  $\mu\text{m}$  amplitudes obviously have several imperfect interfaces (confirmed by optical microscopy). It is well known that imperfect interfaces act like a filter and cause a group delay [13-14]. This group delay is observed as a change in apparent ultrasonic velocity. The values of ultrasonic velocity that appear to be greater than that of the base material (6.3 mm/ $\mu\text{s}$ ) and the decreasing trend of ultrasonic velocities can be attributed to three reasons. The first and most probable being that the exact thickness values are unknown and are estimated from the average thickness after 45 layers of build. The second could be that the acoustoelastic effect is changing the ultrasonic velocity. The third effect could be that as the layer number increases ultrasound travels through more imperfect interfaces thus causing a decreasing quality of build. It is believed that a combination of the above factors is responsible for observed decreasing trends in ultrasonic group velocities. The decreasing trend is not observed in components of lower quality (25, 27  $\mu\text{m}$ ). It is hypothesized that the reason for this is the interaction of the ultrasound echoes from the top of the specimen with those from within



the specimen. These interference effects could distort the measured ultrasonic group velocities especially when the echoes from within the sample are of significant strength. In such cases, calculating the real group velocity pertains to solving the inverse problem of evaluating the part quality given different levels of imperfections within a set of layers. This is beyond the scope of the current work. The interference effects can be further observed through attenuation results.

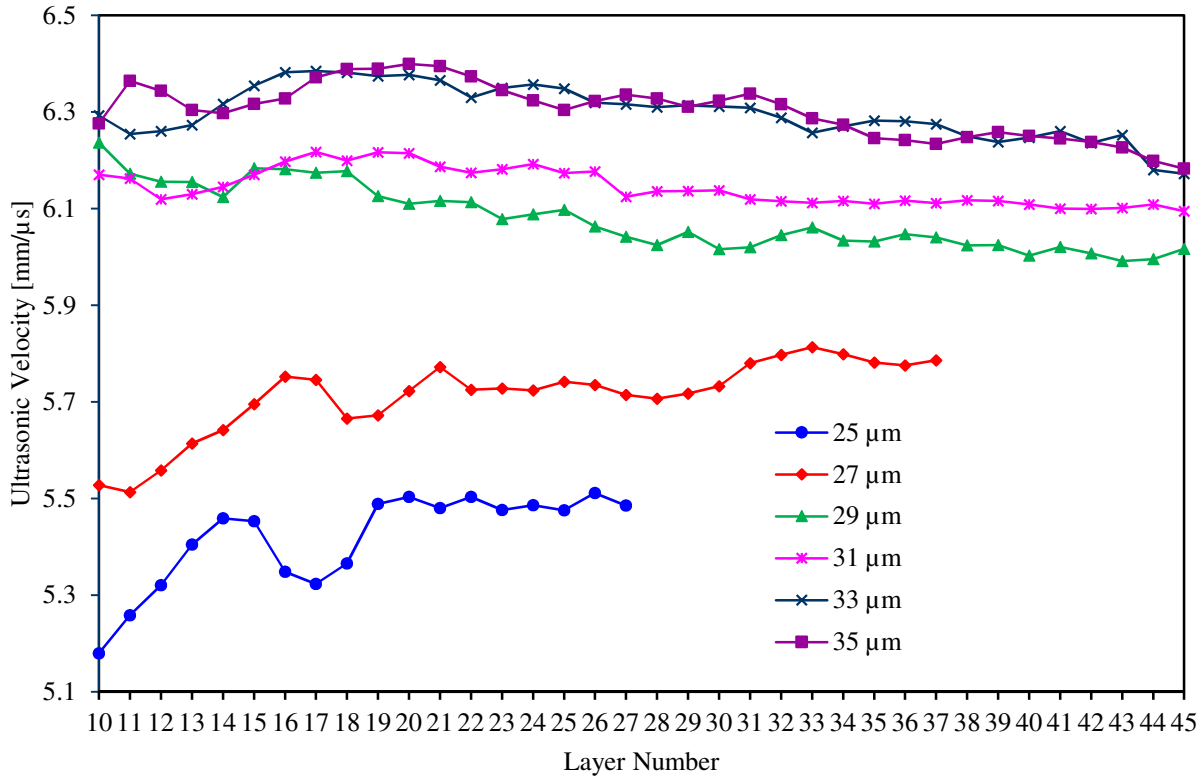


**FIGURE 6.** Ultrasonic group velocity as layers added under various amplitude conditions

### *Ultrasonic Attenuation*

Ultrasonic attenuation is shown in Figure 7. It represents a very interesting phenomenon which occurs due to the periodic nature of the UAM builds. Ultrasonic wave propagation through periodic structures is well studied in layered composites [15]. Due to the periodic nature of the structures and the imperfect interfaces at each layer, there is a small reflection from every single interface of the UAM build. These signals interfere constructively and destructively to form periodically changing amplitudes which also attenuate with increasing number of layers. This effect is most prominent in the low amplitude builds (25 and 27 μm). To a lesser extent, the oscillating periodic nature was also observed for build amplitudes of 29, 31 and 33 μm. The aforementioned phenomenon coupled with the fact that the attenuation loss through the build is lesser as the amplitude increases, implies that each interface reflection is much smaller when the build amplitude is higher. This can be explained by the fact that as the build amplitude is increased until 35 μm the interface quality increases and the UAM layers start behaving like solid aluminum. It is also evident that a bad interface would lead to a higher reflection which would lead to a constructive or destructive interference with the waveforms from the top of the build as subsequent layers are built up. Thus higher attenuation loss and larger oscillations in their relative amplitude

imply bad interfaces while lower attenuation loss and smaller oscillations indicate better bond quality.

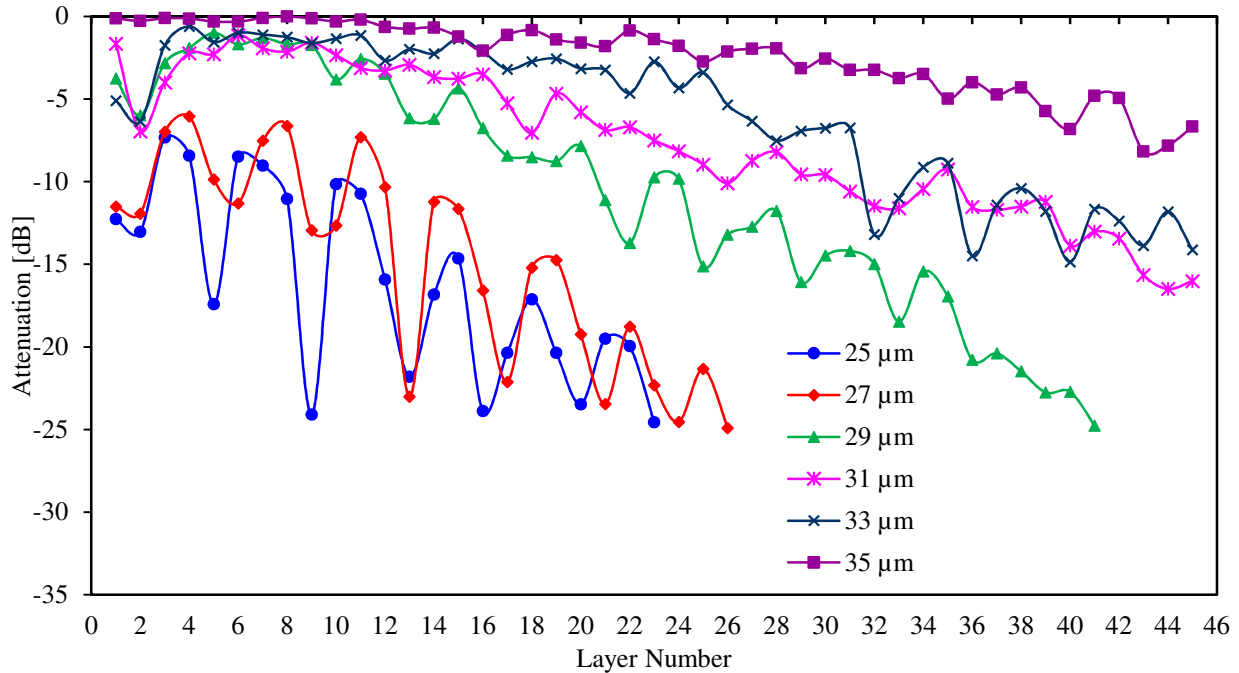


**FIGURE 7.** Relative ultrasonic attenuation of the 3<sup>rd</sup> back wall echo signals due to layer build up

### CONCLUSIONS AND FUTURE WORK

An in-situ ultrasonic non-destructive evaluation system has been developed to monitor bond quality of a build produced by Ultrasonic Additive Manufacturing. An online ultrasonic measurement approach proved to be effective for detecting the inception of small delamination at the base/build interface. This information could be used to adjust the build parameters online to save a component from failure during build. Results from the current in-situ NDE study indicate that linear ultrasonic parameters such as ultrasonic group velocity and attenuation are sensitive to the variations in build amplitude and interface bond quality. Good quality builds exhibited higher ultrasonic velocity, lower attenuation and smaller oscillations in the attenuation values. Fabricated parts with imperfect interface bond conditions lead to lower sound velocities due to signal delay and higher attenuation values because of absorption/scattering through poorly bonded interfaces. The current work shows a qualitative correlation between ultrasonic signatures and UAM build parameters and lays the foundation for a potentially useful in-situ monitoring tool for online closed loop process control.

### ACKNOWLEDGEMENTS

The authors would like to thank Mark Norfolk for access to the SoniLayer R7200 commercial system as well as Hilary Johnson and Brian from Fabrisonics for helping out with the experiments. Joe Vickers and Sudeep Vickram made significant contributions towards work done on the SoniLayer R200 machine. The authors would also like to thank Dr. Peter B Nagy for his valuable advice. Finally, we would like to acknowledge the source of funding from the Office of Naval

Research Grant ONR-BAA #14-004-1110689, Cyber Enabled Manufacturing Systems, Acoustic resonance techniques for online certification and offline qualification of metal based additive manufacturing technologies.

## REFERENCES

1. White, D., & Carmein, D. E. (2002). *U.S. Patent No. 6,463,349*. Washington, DC: U.S. Patent and Trademark Office.
2. Janaki Ram, G. D., Robinson, C., Yang, Y., & Stucker, B. E. (2007). Use of ultrasonic consolidation for fabrication of multi-material structures. *Rapid Prototyping Journal*, 13(4), 226-235.
3. Kong, C. Y., & Soar, R. C. (2005). Fabrication of metal–matrix composites and adaptive composites using ultrasonic consolidation process. *Materials Science and Engineering: A*, 412(1), 12-18.
4. Yang, Y., Ram, G. J., & Stucker, B. E. (2009). Bond formation and fiber embedment during ultrasonic consolidation. *Journal of Materials Processing Technology*, 209(10), 4915-4924.
5. Obielodan, J. O., Ceylan, A., Murr, L. E., & Stucker, B. E. (2010). Multi-material bonding in ultrasonic consolidation. *Rapid prototyping journal*, 16(3), 180-188.
6. Sriraman, M. R., Babu, S. S., & Short, M. (2010). Bonding characteristics during very high power ultrasonic additive manufacturing of copper. *Scripta Materialia*, 62(8), 560-563.
7. Sriraman, M. R., Gonser, M., Fujii, H. T., Babu, S. S., & Bloss, M. (2011). Thermal transients during processing of materials by very high power ultrasonic additive manufacturing. *Journal of Materials Processing Technology*, 211(10), 1650-1657.
8. Kong, C. Y., Soar, R. C., & Dickens, P. M. (2004). Ultrasonic consolidation for embedding SMA fibres within aluminium matrices. *Composite Structures*, 66(1), 421-427.
9. Rieder, H., Dillhöfer, A., Spies, M., Bamberg, J., & Hess, T. (2015, March). Ultrasonic online monitoring of additive manufacturing processes based on selective laser melting. *41ST ANNUAL REVIEW OF PROGRESS IN QUANTITATIVE NONDESTRUCTIVE EVALUATION: Volume 34* (Vol. 1650, No. 1, pp. 184-191). AIP Publishing.
10. Ram, G. J., Yang, Y., & Stucker, B. E. (2006). Effect of process parameters on bond formation during ultrasonic consolidation of aluminum alloy 3003. *Journal of Manufacturing Systems*, 25(3), 221-238.
11. Kong, C. Y., Soar, R. C., & Dickens, P. M. (2003). Characterisation of aluminium alloy 6061 for the ultrasonic consolidation process. *Materials Science and Engineering: A*, 363(1), 99-106.
12. Papadakis, E. P. (1968). Ultrasonic attenuation in thin specimens driven through buffer rods. *The Journal of the Acoustical Society of America*, 44(3), 724-734.
13. Nagy, P. B. (1992). Ultrasonic classification of imperfect interfaces. *Journal of Nondestructive evaluation*, 11(3-4), 127-139.
14. Nagy, P. B. (1991). Ultrasonic detection of kissing bonds at adhesive interfaces. *Journal of Adhesion Science and Technology*, 5(8), 619-630.
15. Rokhlin, S.I., Chimenti, D. E., & Nagy, P. B. (2011). *Physical ultrasonics of composites*. Oxford University Press.